ACS OMEGA

Open Access

http://pubs.acs.org/journal/acsodf

Article

Coomassie Brilliant Blue Induces Coiled-Coil Aggregation in Lysozyme at pH 7.4 by Hydrophobic and Electrostatic Forces

Ajamaluddin Malik,*,⊥ Javed Masood Khan,⊥ Priyankar Sen, Abdulaziz Alamri, Rohit Karan, and Arnold Emerson I

Cite This: *ACS Omega* 2025, 10, 1829−1838

Read Online

ACCESS | Metrics & More | Article Recommendations | Supporting Information

ABSTRACT: Several neurodegenerative diseases are associated with the deposition of amyloid fibrils. Although these diseases are irreversible, knowing the aggregation mechanism is useful in developing drugs that can arrest or decrease the aggregation rate. In this study, we are interested in investigating the effect of Coomassie brilliant blue (CBB G-250) on the aggregation of hen egg white lysozyme (HEWL) at pH 7.4. Various biophysical techniques have been used, such as turbidity, Rayleigh light scattering (RLS) kinetics, far-UV circular dichroism (CD), field emission scanning electron microscopy (FESEM), and transmission electron microscopy (TEM) imaging. The turbidity data indicated that CBB (≥0.1 mM) induces aggregation in HEWL at pH 7.4. The aggregation kinetics caused by CBB are quick without a lag phase and are dependent on the CBB concentration. The far-UV CD data revealed that the CBB-induced aggregated samples had lost their CD signals without exhibiting a shift in the spectrum position. Sodium chloride and ammonium sulfate show little effect on the CBB-induced aggregates, but alcohol such as methanol, ethanol, and 2-propanol could reverse the aggregation. Overall, this study aims to better understand the mechanism underlying CBB-induced aggregation and keep in mind that CBB employed in laboratories can alter the protein structure. We report the aggregation of a natural protein due to coiled-coil formation induced by a dye at physiological pH and temperature conditions. This finding has high value because several dyes are used for diagnostic and therapeutic purposes, and coiled-coil formation is closely related to infection mechanisms and nanoparticle-based drug deliveries.

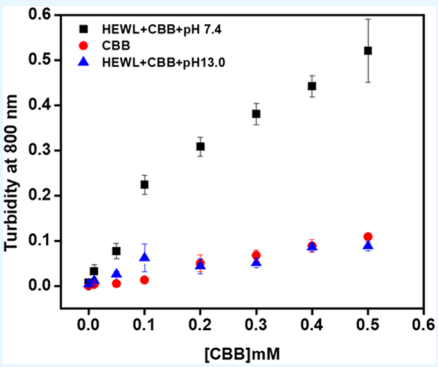

INTRODUCTION

Several disorders, including type II diabetes, Parkinson's disease, Alzheimer's disease, and Huntington's disease, have been linked to the misfolding and aggregation of proteins.[1] One of the fundamental problems in multidisciplinary sciences is determining how proteins and peptides form amyloid fibrils *in vitro* and *in vivo*. The amyloid fibril relates to insoluble protein or peptide aggregates and has an expanded cross-β-structure.[2] It is widely known that the accumulation of partially folded/unfolded intermediate states is a key point for the initiation of protein aggregation.[3] It was reported that the formation of protein aggregates is significantly influenced by the pH of the solution, salt concentration, protein concentration, and shear stress.[4,5] It was found that many proteins that may not cause any amyloid disorder can produce ordered amyloid-like aggregates too. The amyloid formation was found to be a generic property of all of the proteins.[6] Numerous small molecules are also known to trigger aggregation in addition to environmental variables like pH, temperatures, salt concentrations, and protein concentration.[4,7,8] It has been discovered that anionic molecules, particularly sulfated glycosaminoglycans, i.e., heparin sulfate, induce aggregation in tau protein. This is likely due to their assistance in breaking down the nucleation barrier on the aggregation pathway.[9] Several dyes are known to induce protein aggregation at physiological and acidic pH.[10,11] However, the impact of CBB on the protein structure and aggregation has been poorly studied. CBB has been found to act as a chemical chaperone as well as a protein aggregation inducer.[12−15]

Several dyes are used for diagnostic and therapeutic purposes: Congo red,[16] thioflavin T,[17] tartrazine,[18] fluorescein,[19] CBB,[20] methylene blue,[21] and Trypan blue[22] are a few of them. CBB is a widely employed dye for protein staining. Usually, it is conventionally used in gel electrophoresis, but recent studies have uncovered a fascinating aspect of its interaction with proteins in solution.[23] CBB is a triphenylmethane dye, and the structure is shown in Figure 1A. This dye has a strong propensity to establish electrostatic interactions with protonated basic amino acids and form hydrophobic interactions with aromatic residues of the proteins.[24] This dye does not bind to polyacrylamide with high affinity but can

Received: November 10, 2024
Revised: December 12, 2024
Accepted: December 13, 2024
Published: December 21, 2024

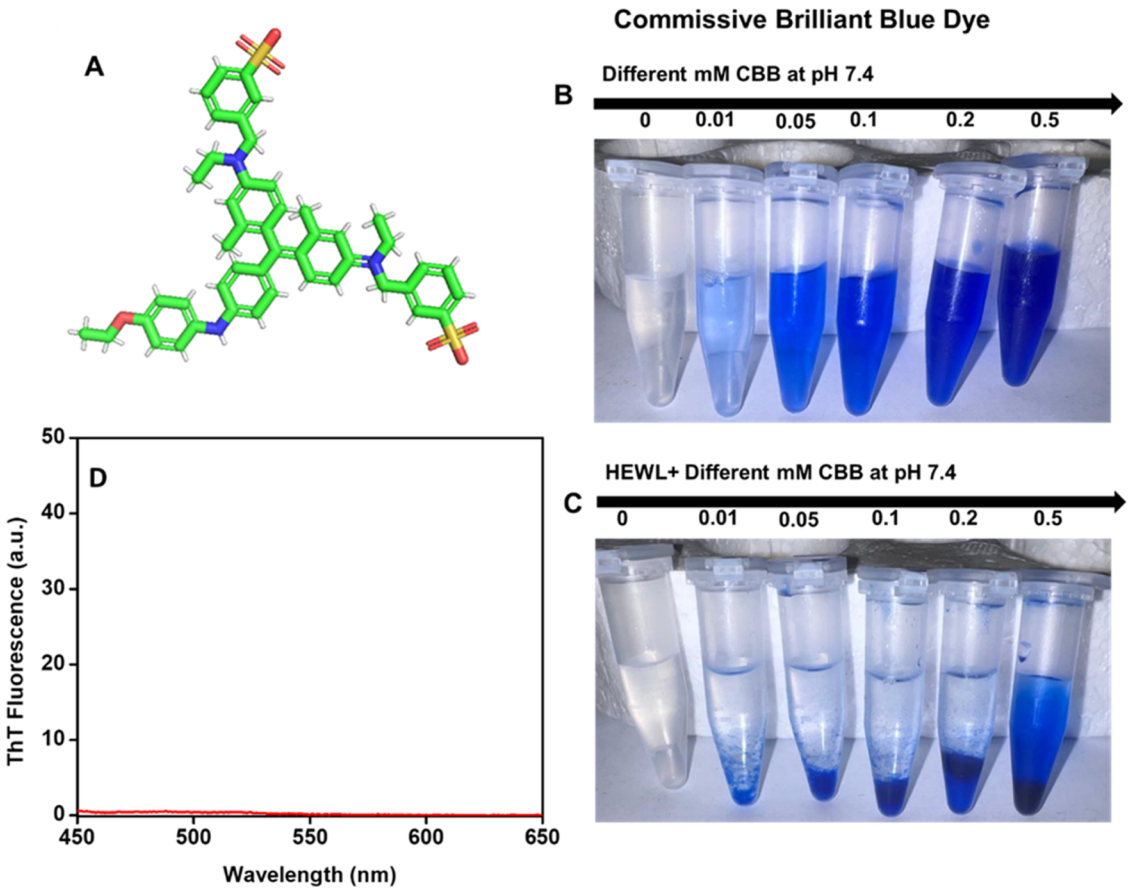

Figure 1. Panel A shows the chemical structure of Coomassie brilliant blue G-250. Carbon atoms are represented in green, nitrogen in blue, oxygen in red, and sulfur in yellow. Panel B shows the various concentrations of CBB (in mM) without HEWL at pH 7.4, which served as a control. Panel C shows the photograph of HEWL (0.2 mg mL^{-1}) treated with different concentrations of CBB (in mM) at pH 7.4. Panel D shows ThT fluorescence spectra of HEWL without CBB at pH 7.4.

penetrate the gel matrix and bind with low affinity. It has the ability to interact electrostatically with protein by noncovalent interactions. The CBB binds to proteins, including wool (keratin), to form a protein−dye complex.[25] Interestingly, the interaction of the CBB with the protein was not explored in detail. The binding properties of CBB with one of the model proteins, hen egg white lysozyme (HEWL), have been thoroughly studied in this work.

HEWL has been subjected to intense investigation due to its well-defined structure and links in familial lysozyme systemic amyloidosis.[26] HEWL, a monomeric protein consisting of 129 a.a. residues with a molecular weight of 14.3 kDa, is a well-known food preservative due to its effective antimicrobial activity.[27] In terms of structure, HEWL is a helix-rich protein (with 30% α-helix), has four disulfide bonds, and exhibits a high degree of structural and sequence homology to the human lysozyme.[28] HEWL is susceptible to fibrillation in a hot and acidic environment.[29,30] Additionally, denaturants like guanidine hydrochloride and solvents like ethanol promote aggregation.[31,32] This is why HEWL has been widely chosen as a model protein in aggregation and amyloid fibrillation research.

The current work aims to explore the molecular mechanism of the aggregation of HEWL caused by the CBB. We have also seen the effect of slats and solvents in the CBB-induced aggregation process. Identifying the driving forces and structural alterations associated with the CBB-induced HEWL aggregation process is also interesting. The study will improve our understanding of protein−dye interactions and may have larger ramifications for disciplines such as biochemistry and biophysics.

MATERIAL AND METHODS

Materials. Hen egg white lysozyme (HEWL) (lot#BCBM4658 V) and Coomassie brilliant blue (CBB) dye (lot#SHBL0658) were purchased from Sigma- Chemicals Co. (St. Louis, MO). All of the reagents used in this study were of analytical grade.

Solution Preparation. HEWL powder (5.0 mg mL^{-1}) was dissolved in 20 mM phosphate buffer at pH 7.4 and centrifuged at 13,000 rpm for 15 min at 4 °C to remove insoluble aggregated protein. HEWL concentration was determined spectrophotometrically using an extinction value ($E^{0.1\%}$) of 2.64 mg mL^{-1} cm^{-1} at 280 nm.[33] The 20 mM CBB dye stock was made in Milli-Q (Millipore Corp., Bedford, MA) water using weight/volume techniques. Thioflavin 10 mM stock solution was prepared in deionized water. All of the solutions used in this study were freshly prepared.

Turbidity Measurements. The turbidity measurements of CBB-induced aggregation of HEWL at pH 7.4 and 13 were performed. The turbidity of the aggregated samples was measured by a Cary 60 UV−vis Spectrophotometer (Agilent Technologies, Santa Clara, CA). The turbidity of HEWL (0.2 mg mL^{-1}) without CBB and with various concentrations (0.0−

https://doi.org/10.1021/acsomega.4c10216
ACS Omega 2025, 10, 1829−1838

3.0 mM) of CBB was measured by recording the absorbance at 800 nm in an arbitrary unit (au). CBB showed strong absorption below 750 nm; hence, turbidity measurements for all samples were carried out at 800 nm. Prior to measurements, all of the samples treated without and with different concentrations of CBB were incubated overnight. The absorbance at 800 nm was plotted against the CBB concentrations.

Effects of different concentrations of salts (NaCl and $(NH_4)_2SO_4$) and solvents (methanol, ethanol, and 2-propanol) were also seen on CBB-induced HEWL aggregation. The absorbance at 800 nm was plotted against different salt concentrations, and different percentages of solvents on CBB-induced HEWL aggregates were plotted.

The ThT spectra of HEWL (0.2 mg mL^{-1}) treated with 10 μM ThT at pH 7.4 were recorded by exciting at 440 nm, and data was collected from 450 to 600 nm on a Cary Eclipse spectrofluorometer.

Aggregation Kinetics Measurements. Rayleigh light scattering (RLS) was conducted to test the CBB dye-induced HEWL aggregation at pH 7.4. Light scattering at 800 nm was monitored in the presence of different concentrations (0.0, 0.01, 0.05, 0.1, 0.2, and 0.5 mM) of CBB dye with 0.2 mg mL^{-1} HEWL in the 3.0 mL cuvette. The different CBB dye concentrations were added every 100 s. The light scattering was measured on a Cary Eclipse Fluorescence Spectrofluorometer after excitation at 800 nm and measurement of the emission at 800 nm. The emission at 800 nm was plotted against time (in seconds). The excitation and emission slit widths were 1.5 and 2.5 nm, respectively.

The kinetics of CBB-induced HEWL aggregates was also tested in the presence of solvents. The HEWL was pretreated with 0.2 mM CBB and incubated overnight. Then, different percentages of solvents were added, and the scattering intensity was measured at 800 nm with respect to time. The CBB-treated HEWL was further studied in the presence of increasing concentrations of cosolvents like methanol, ethanol, and 2-propanol by light scattering at 800 nm.

Circular Dichroism Measurements. Far-UV CD measurements were carried out on a Chirascan-Plus spectropolarimeter (Applied Photophysics, UK) to examine the changes in the HEWL secondary structure in the absence and presence of varying concentrations of CBB dye at pH 7.4. Before far-UV CD measurements, the HEWL solution (0.2 mg mL^{-1}) alone and with different concentrations of CBB dye was incubated overnight at room temperature. The spectra of all of the samples were scanned from 190 to 260 nm with a quartz cuvette of 0.1 cm path length.

The spectropolarimeter was continuously purged with grade 5 nitrogen gas throughout the experiments. All spectra were subtracted from their respective blanks, and each spectrum was taken as an average of three scans. The effect of two salts (NaCl and $(NH_4)_2SO_4$) on the secondary structure of preformed aggregates (HEWL treated with 0.2 mM CBB dye) was seen. The effect of solvents, including methanol, ethanol, and 2-propanol, was seen on the preformed CBB-induced HEWL aggregates.

Field Emission Scanning Electron Microscopy (FESEM). Samples were prepared as per the protocol in the "sample preparation" section above. Then, they were kept in the −80 °C deep freezer for 24 h. Then, 0.5 mL of samples were freeze-dried in a freeze-dryer (Christ Freeze-Dryer, beta 1−8 LD plus) for 24 h to remove all of the moisture. A FESEM (Thermo Fisher FEI QUANTA 250 FEG) at VIT Vellore central facility, with an achievable resolution of 1.2 nm at 30 kV and 2.3 nm at 1 kV with beam deceleration in high vacuum using the in-column detector, has been used to study samples. The magnification was 10,000×, and the voltage was 20 kV.

Transmission Electron Microscopy (TEM). The JEOL electron microscope (JEM-1011 model) was used for capturing TEM images of CBB-treated HEWL samples in the presence and absence of 50% ethanol while operating at an accelerating voltage of 80 kV. The effect of CBB on the morphology of HEWL aggregates in the absence and presence of ethanol was investigated using ten microliter samples of 0.2 mg/mL HEWL. The samples were put on a 200-mesh copper grid. After a 2 min incubation period, the grids were cleansed of leftover buffer and negatively stained with 2% uranyl acetate. After being air-dried, the samples on the grids were analyzed under the TEM.

RESULTS

Aggregation Reaction in Microcentrifuge Tubes. Figure 1B,C depicts the blank (CBB without HEWL) and visible clumps formed when HEWL was incubated with CBB in microcentrifuge tubes. Figure 1B shows the different concentrations of CBB at pH 7.4 without HEWL. CBB was not aggregating and remained soluble in the buffer at pH 7.4. However, Figure 1C shows the development of visible aggregates of HEWL in the presence of different concentrations of CBB at pH 7.4. In the control experiment, ThT dye did not bind with HEWL at pH 7.4, indicating that HEWL was soluble in the absence of CBB.

Turbidity Measurements of CBB-Induced HEWL Aggregation. The turbidity at 800 nm was used to evaluate the extent of HEWL aggregation in the presence of CBB dye at pH 7.4. As shown in Figure 2, there was no turbidity in the HEWL solution without CBB, demonstrating that HEWL does not aggregate at physiological pH. However, HEWL treated with 0.1 to 0.5 mM CBB dye showed an increase in turbidity, confirming that HEWL was aggregated in the presence of CBB dye. Moreover, HEWL incubated with below 0.1 mM dye concentration demonstrated no turbidity, suggesting that

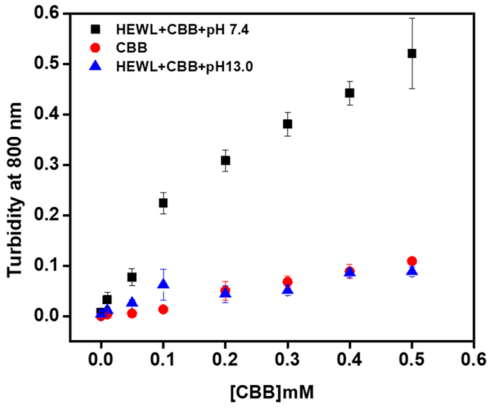

Figure 2. Effects of CBB on HEWL aggregation at pH 7.4 and 13. The turbidity of HEWL at pH 7.4 (■) and pH 13 (▲) with different CBB concentrations in millimolars was recorded at 800 nm. The turbidity of CBB without HEWL (●) was also recorded at 800 nm at pH 7.4. HEWL concentrations were fixed at 0.2 mg/mL in all of the samples.

https://doi.org/10.1021/acsomega.4c10216
ACS Omega 2025, 10, 1829−1838

HEWL did not form aggregates at these concentrations. Notably, the turbidity progressively increased from 0.1 to 0.5 mM dye concentrations, which signified that the HEWL formed aggregates in response to dye concentrations. We could not measure turbidity for further (>0.5 mM) dye concentrations because the dye starts absorbing at this wavelength. The turbidity results suggest that HEWL forms aggregates in the presence of concentrations above 0.1 mM dye concentrations, and HEWL remains soluble below 0.1 mM dye concentrations at physiological pH.

Kinetics for CBB-Induced HEWL Aggregation. Rayleigh scattering is extensively used to study the kinetics and extent of protein aggregation in solution. The light scattering of the solution was found to be significantly very high when the protein became aggregated.[34] To test the kinetics of HEWL aggregation in response to different doses of CBB at pH 7.4, the kinetics of HEWL aggregation were examined by monitoring time-dependent changes in light scattering intensity, and data are presented in Figure 3. This figure

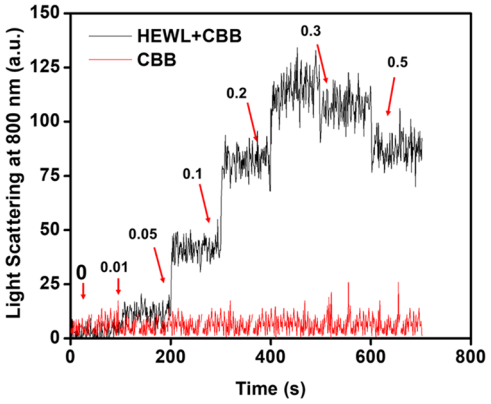

Figure 3. Aggregation kinetics of HEWL in the presence of different doses of CBB were measured by light scattering measurements. HEWL (0.2 mg/mL) treated without and with different concentrations of CBB in mM at pH 7.4 (black line) are plotted in the figure. The light scattering of the sample containing different concentrations of CBB without protein (red line) was also measured at pH 7.4. The change in light scattering was measured with respect to time in seconds.

displayed a single kinetic trace, demonstrating that experiments were conducted in a 3 mL cuvette using various doses of the CBB dye. A different dose of dye was added every 100 s, and scattering at 800 nm was captured with respect to time in seconds. From the kinetic trace, it was clear that the HEWL without and with 0.01 mM CBB dye displayed no scattering for up to 100 s, indicating that the HEWL does not aggregate at these conditions. However, upon the addition of 0.05, 0.1, and 0.2 mM of CBB, the light scattering progressively increased many folds, and the reaction did not last for 400 s. Afterward, 0.3 and 0.5 mM CBB were added to the same sample, and the light scattering did not increase. Scattering was found to be a little bit low, and the kinetic reaction was saturated. The possibility of low light scattering at higher concentrations of CBB dye may be the formation of bigger-sized aggregates. The most interesting observation was that HEWL immediately formed aggregates after mixing with dye and that there was no lag phase in the kinetic reaction, indicating that HEWL was converted to larger aggregates. This kinetic data recommended that the HEWL aggregation was dependent on CBB dose and thus did not have a lag phase.

Secondary Structure Modification Measurements by Far-UV CD. To evaluate the modification in the secondary structure of HEWL proteins in the presence of CBB dye at physiological pH, Figure 4 shows the far-UV CD spectra of

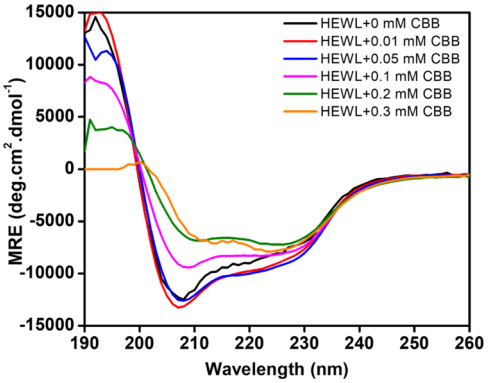

Figure 4. HEWL secondary structure modifications were measured by far-UV CD. HEWL (0.2 mg/mL) at pH 7.4 was incubated with different concentrations of CBB dye. Far-UV CD spectra of HEWL (0.2 mg/mL) in the absence of CBB (black line) and in the presence of 0.01 (red line), 0.05 (blue line), 0.1 (pink line), 0.2 (green line), and 0.3 (orange line) mM CBB at pH 7.4.

HEWL without and with different concentrations of the CBB dye at pH 7.4. The far-UV CD spectra of HEWL without dye show two negative ellipticity at 208 and 222 nm. The negative ellipticity at 208 nm was slightly higher than the negative ellipticity at 222 nm, a typical characteristic of the $\alpha + \beta$ class protein.[35] The far-UV CD spectra of HEWL with 0.01 and 0.05 mM CBB showed that the negative ellipticity at 208 and 222 nm was slightly increased, confirming gain in the α-helical structure (Table 1). However, with the addition of 0.1, 0.2, and

Table 1. Percent Secondary Structural Changes were Determined Using the K2D2 Method under Various Conditions

s. no.	conditions	α-helix	β-sheet
1	HEWL at pH 7.4	23.7	26.2
2	HEWL + 0.01 mM CBB	25.57	20.69
3	HEWL + 0.05 mM CBB	25.57	20.69
4	HEWL + 0.1 mM CBB	19.69	31.52
5	HEWL + 0.2 mM CBB	14.98	34.94
6	HEWL + 0.3 mM CBB	14.98	34.94

0.3 mM CBB, the negative ellipticity of far-UV CD has drastically reduced, and the peak at 208 nm was shifted slightly. Interestingly, the peak at 222 nm has not shifted, but the negative peak ellipticity was reduced drastically. These observations suggest that HEWL was aggregated in the presence of 0.1, 0.2, and 0.3 mM CBB at pH 7.4.

Effect of Salts on CBB-Induced HEWL Aggregates. We examined the effects of two salts (NaCl and $(NH_4)_2SO_4$) on the CBB-induced HEWL aggregation reaction. Figure 5A shows the turbidity profile of HEWL with 0.2 mM CBB dye and different concentrations of both salts. The turbidity profile indicated that none of the salts affected the aggregation. Similarly, the secondary structure of aggregated HEWL was not affected by the salts as well (Figure 5B,C). The shape of

https://doi.org/10.1021/acsomega.4c10216
ACS Omega 2025, 10, 1829−1838

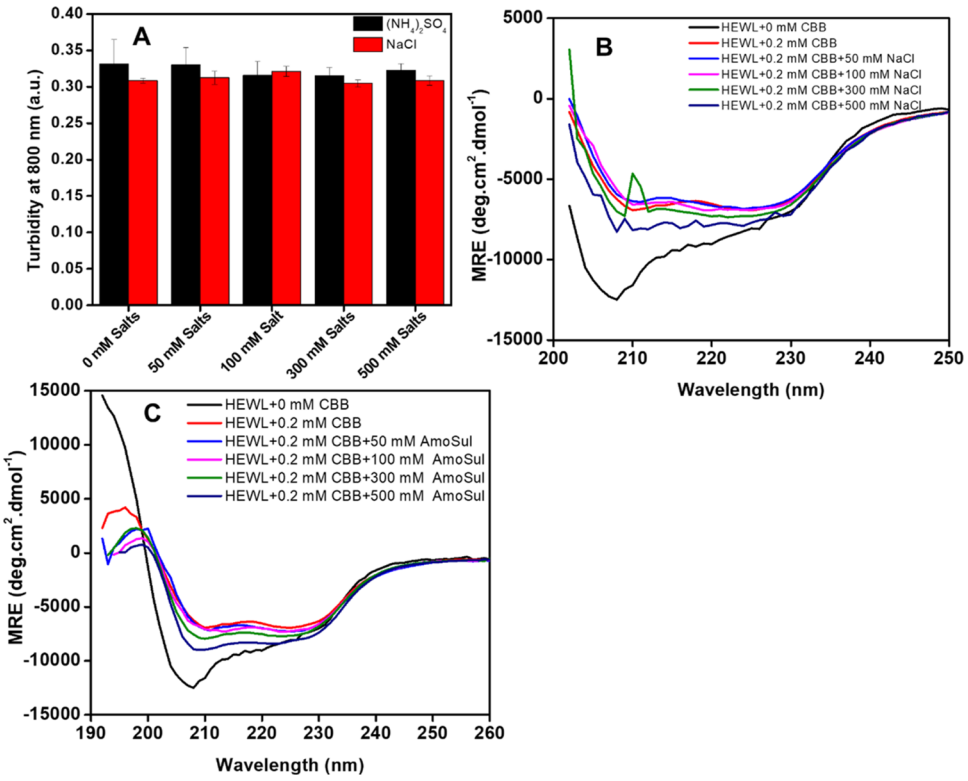

Figure 5. Effects of salts on the preformed aggregates (0.2 mg/mL HEWL + 0.2 mM CBB) at pH 7.4. (A) Turbidity profile of the aggregates at different concentrations of NaCl (Red bar) and $(NH_4)_2SO_4$ (Black bar). Secondary structure modifications of preformed HEWL aggregates in the presence of NaCl (B) and $(NH_4)_2SO_4$ (C) at pH 7.4.

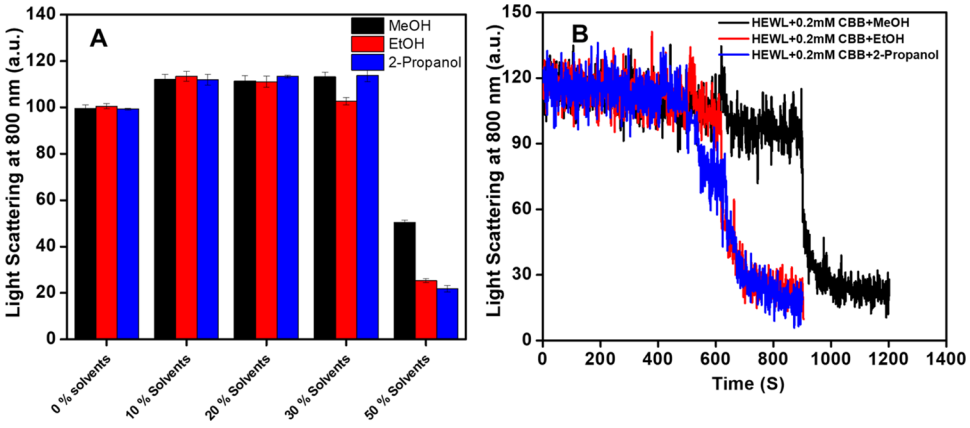

Figure 6. Effects of methanol, ethanol, and 2-propanol on preformed HEWL aggregates at pH 7.4. (A) The light scattering profile of preformed (HEWL (0.2 mg/mL) + 0.2 mM CBB dye) aggregates in the presence of different concentrations of alcohols at pH 7.4. (B) The light scattering kinetics of preformed HEWL aggregates and exposure of different concentrations of alcohols at pH 7.4.

the CD spectrum of HEWL incubated with 0.2 mM CBB remained the same in the presence of NaCl (Figure 4B) and $(NH_4)_2SO_4$ (Figure 4C) with a marginal increase in ellipticities with the salt concentrations. The turbidity and far-UV CD results suggest that these salts did not disintegrate the CBB-induced HEWL aggregates. However, a marginal change in the secondary structure was evident.

Effects of Alcohols on CBB-Induced HEWL Aggregation. Alcohols are nonpolar. The effects of alcoholic cosolvents, i.e., methanol, ethanol, and 2-propanol, on CBB-induced HEWL aggregates have been studied. Figure 6A shows the turbidity profile of HEWL incubated with 0.2 mM CBB dye and different percentages of alcohols. The turbidity was slightly increased in the presence of 10−30% alcohol. However, in the presence of 50% alcohol, the light scattering was found to be decreased, and maximum decrement was found in the presence of ethanol and 2-propanol.

The aggregation kinetics of HEWL treated with 0.2 mM of CBB dye was studied in the presence of 10−50% alcohols, and data is shown in Figure 6B. The kinetic results suggest that the presence of 50% ethanol and 2-propanol led to a rapid disappearance of the preformed aggregates. However, when 50% methanol was added, the aggregates took a bit more time to solubilize. The turbidity and the kinetic results suggest that CBB-induced HEWL aggregates were solubilized in the

https://doi.org/10.1021/acsomega.4c10216
ACS Omega 2025, 10, 1829−1838

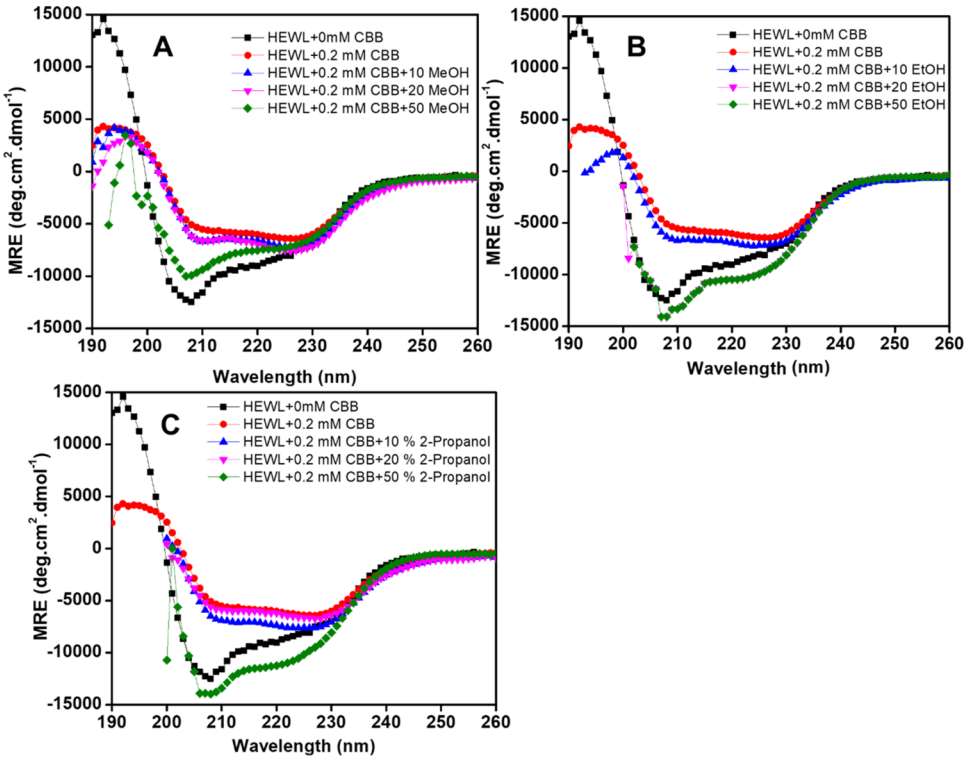

Figure 7. Secondary structure modification of HEWL treated with 0.2 mM CBB in the presence of different percentages of methanol (A), ethanol (B), and 2-propanol (C) at pH 7.4. Every spectrum was labeled in the inset. HEWL concentration was 0.2 mg/mL in all of the samples.

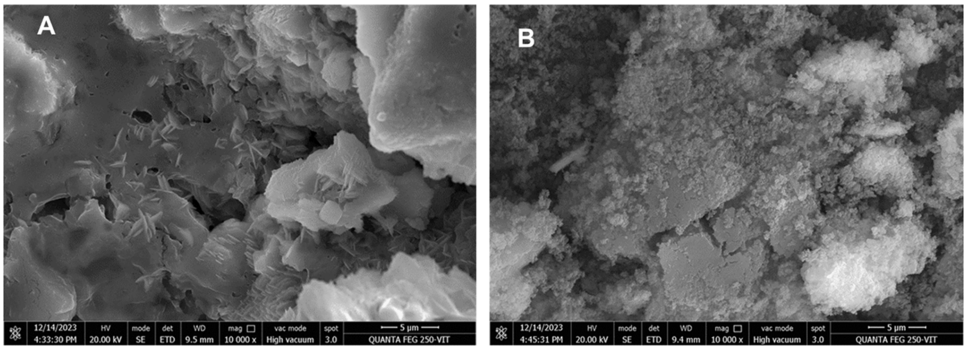

Figure 8. Field emission scanning electron micrograph of 0.2 mM CBB-treated HEWL aggregates in the absence (A) or presence (B) of 50% ethanol at pH 7.4 and 298 K.

presence of all three alcohols, but ethanol and 2-propanol were more effective than methanol.

Effect of Alcohols on the Secondary Structures of CBB-Induced HEWL Aggregates. The conformational changes of CBB-induced HEWL aggregates were further investigated in the presence of various concentrations of alcohols by far-UV CD. The far-UV CD spectra of HEWL in the absence and presence of dye and alcohols are shown in Figure 7A–C. The HEWL without and with 0.2 mM CBB dye were shown, and all three figures have similar spectra, as we have discussed in Figure 4. However, the negative ellipticity did not change much in the presence of 10% of all of the alcohols. In the presence of 20% ethanol (Figure 7B) and 2-propanol (Figure 7C), the dye-treated samples' negative ellipticity significantly increased and eventually reached the negative ellipticity of the dye-free HEWL. Interestingly, it was also seen that in the presence of 50% methanol (Figure 7A), the negative ellipticity slightly increased but did not reach the negative ellipticity of dye-free HEWL samples, which confirms that the HEWL was still aggregated in the solution. Overall, far-UV CD results also suggest that ethanol and 2-propanol were more effective in dye-induced HEWL aggregate solubilization than methanol. The solvent data suggest that the observed solubilization of CBB-induced HEWL aggregates may be caused by a hydrophobic interaction.

The $\theta_{222}/\theta_{208}$ ratio of the UV CD data mentioned above has been registered in Supporting Table S1. If the ratio is <0.9, it indicates isolated helices, as found in native HEWL, but if the ratio is >1.0, it indicates coiled-coil formation. In the presence of 0.2 mM CBB, the secondary structure HEWL becomes a coiled coil instead of $\alpha + \beta$. Interestingly, aggregates also formed in the same stage. In the presence of salts, neither aggregates disappear nor coiled coil. However, in the presence of 50% (v/v) methanol and 30% (v/v) and 50% (v/v) ethanol and 2-propanol, respectively, isolated helices reappear. Interestingly, the disappearance of aggregates also occurs in

https://doi.org/10.1021/acsomega.4c10216
ACS Omega 2025, 10, 1829−1838

the same range, but it seems that the disappearance of coiled coil occurs first, followed by the disappearance of aggregates.

FESEM Results. The HEWL FESEM data matched previously reported HEWL micrographs (data not shown).[36,37] The FESEM result (Figure 8) also supports the results of far-UV CD. In the presence of CBB, some aggregated structures were visible.[38,39] But interestingly, in the presence of 50% ethanol, the structures disappear.

TEM Imaging. High-resolution imaging and direct monitoring of aggregate morphology were performed through transmission electron microscopy (TEM) imaging of the CBB-induced aggregation of HEWL in the absence and presence of ethanols. Aggregated structures were found in 0.2 mM CBB-treated HEWL (Figure 9A), while disintegrated morphology of CBB-treated HEWL aggregate was found in the presence of 50% ethanol (Figure 9B).

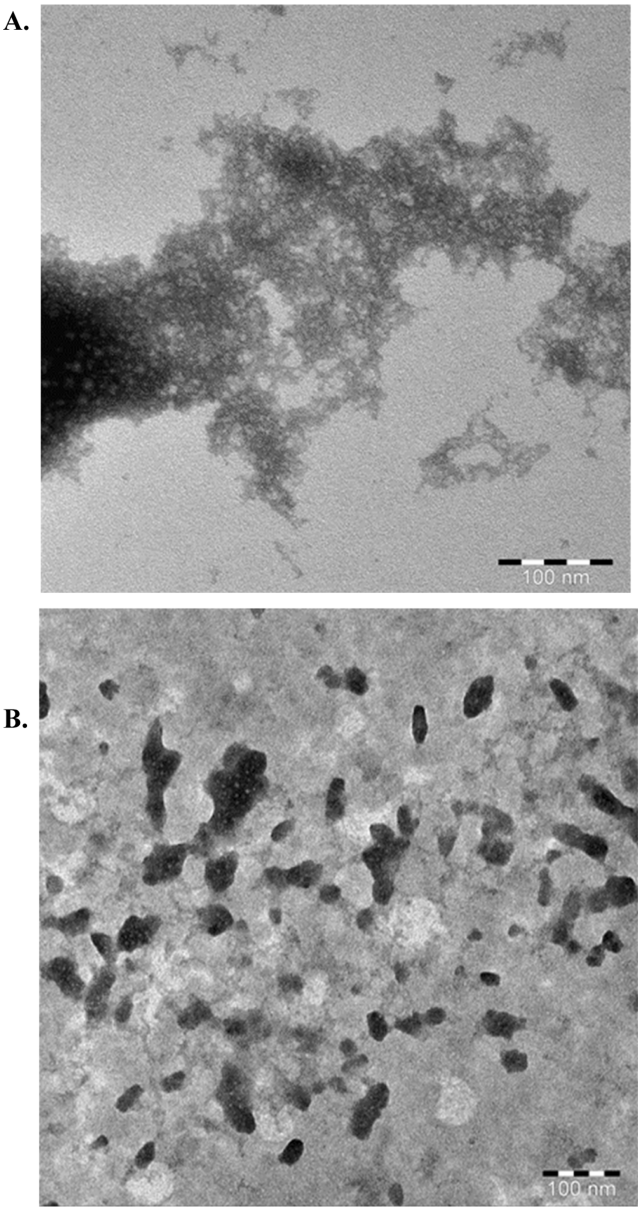

Figure 9. Transmission electron microscopic image of 0.2 mM CBB-treated HEWL aggregates in the absence (A) or presence (B) of 50% ethanol at pH 7.4.

DISCUSSION

Coomassie brilliant blue G-250 is a well-known dye that binds specifically to proteins and helps in protein quantification through a method called the Bradford assay. Both CBB G-250 and R-250 were found to induce nonconventional self-assembly in α-synuclein.[13] Lysozyme is known for forming aggregates under non-native conditions. Due to its compact structure and disulfide bonds, its secondary structure remains stable at pH 7 to 4. Although, at pH 2, it retains its secondary structure, even in the presence of a small amount of alcohol, it misfolds and forms insoluble aggregates. However, at high concentrations of alcohols, it retains its native secondary structure at pH 4 and 7.[40]

Lysozyme is a single-chain protein with 129 residues. It folds into a compact structure with 5 α helices, one 3−10 helix, and 5 β strands. The α helices of lysozyme are spatially positioned close to each other, which probably helps them arrange in a coiled coil during aggregation. The $\theta_{222}/\theta_{208}$ ratio gives information on the chance of the α helices being assembled in a coiled-coil structure.[41−44] A ratio of 0.9 or less indicates that helices were isolated as in the native state of lysozyme. If the ratio is greater than 1.0, it indicates that a coiled coil has formed.[41,45] The presence of heptad (seven-residue motif: a repeated pattern hxxhcxc having h (hydrophobic amino acid) and c (charged amino acid)) is the hallmark of coiled coils, which is absent in HEWL.[46] However, other studies suggested that nonheptad motifs can assemble in a Coiled-coil structure.[47]

Based on the dielectric constant, the relative polarity of 2-propanol (0.546) is less than that of ethanol (0.654) and methanol (0.762).[48] At comparative volumes, 2-propanol and ethanol show a better chance of reversal of aggregation and native-like helicity than methanol. An increase in hydrophobicity in solvent disrupts intermolecular coiled coils in HEWL that were bridged by CBB, hence increasing solubility.

Coiled coils are α-helical super secondary structures mediating protein−protein interactions, oligomerization, and other functions through the coiling belonging to the same or different polypeptide chains.[49] In principle, α-helical and β-sheet structures in different protein domains could also act in parallel to mediate aggregation.

Coiled-coil domains can mediate protein interactions and multimerization. Mutations that disrupt coiled coils impair aggregation, and mutations that enhance coiled-coil propensity promote aggregation in Q/N-rich prions and polyQ proteins.[45] A mutation that increases the length of PolyQ stretches results in an enhanced coiled coil and aggregation. It results in Huntington's disease, an inherited disorder.[50] Many peptides' coiled coils were found to bind with polynucleotides also.[51] Our earlier work showed that alkaline-denatured BSA aggregates in the presence of trifluoroethanol with coiled-coil formation.[52] BSA, which is otherwise predominantly an α-helical structure devoid of β-sheets, loses its secondary structure and acquires random coil conformation at extreme alkaline pH. But, in highly hydrophobic alcohol, the denatured protein gets withdrawn from the alkaline solvent and reacquires α-helical coils following Anfinsen's dogma. However, the presence of a highly hydrophobic environment and a non-native refolding results in intrapolypeptide and interpolypeptide coiled-coil formation and eventually aggregation.

CBB possesses a net (−1) charge at neutral pH, but HEWL has a net positive charge due to high lysine content.[53] The

https://doi.org/10.1021/acsomega.4c10216
ACS Omega 2025, 10, 1829−1838

surface of HEWL is relatively hydrophobic, and the CBB is hydrophobic due to bulky aromatic groups. Previous studies have shown that proteins like trypsin, which has basic residues and is widely separated in its sequence, show lesser binding to CBB in comparison to HEWL, which has basic amino acids and patches in the vicinity of nonpolar residues. It seems the charge interaction takes place first, proceeding by hydrophobic interaction to form CBB-HEWL complexation.[24] The FESEM and TEM micrographs also supported the hypothesis. HEWL, in the presence of CBB, forms aggregates. But interestingly, in the presence of 50% ethanol, those structures disappear.

CONCLUSIONS

CBB is a Y-shaped dye made up of aromatic benzene rings and two negatively charged sulfonic groups at pH 7.4 situated at the edges. When it binds to HEWL, the sulfonic groups are neutralized by Arg 112 and Arg 73 and become susceptible to hydrophobic interactions with neighboring HEWL-CBB complexes. Thus, this results in aggregation. HEWL is an $\alpha + \beta$ protein; its α-helices and β-sheets remain assembled apart from each other. When CBB forms complexation with HEWL, it engages with the β-rich domain, leaving the α-rich domain away from the interaction. It liberates α-rich domains to form interstrand coiled coils, as they are forced to ensemble together due to the formation of aggregates. In the formation of coiled coils, some role, although marginally, was played by charged groups of the α-helices, as there was little loss of interactions in the presence of high concentrations of salt. However, the major blow to aggregates takes place in the presence of alcohol, which disrupts the interaction of CBB- HEWL complexes by dissolving hydrophobic interactions.

Nonamorphous aggregates mostly occur due to the systematic cross-β sheet linkages, commonly called amyloid formation. On the contrary, another systematic aggregation takes place with coiled coils. Although they are fewer in number in comparison to amyloids, their roles are significant. Many connective tissues and transmembrane proteins form coiled coils. The efficacy of many diseases depends on the formation of coiled coils to penetrate cell membranes. Recently, a lot of interest has emerged in exploiting the coiled-coil structure in nanotechnology, specifically as a drug delivery apparatus. Attempts are made to create coiled-coil IBs to be used as nanobots. Coiled-coil HEWL aggregates have potential applications due to their simple structure and well-known background. Similarly, CBB is also a nontoxic and well-studied stable molecule. This is the first report of a stable and switchable coiled-coil aggregation of a simple protein that remains stable in a large range of pH and that is induced by a cost-effective dye with a good potential for clinical exploitation.

ASSOCIATED CONTENT

Supporting Information

The Supporting Information is available free of charge at https://pubs.acs.org/doi/10.1021/acsomega.4c10216.

$\theta_{222}/\theta_{208}$ ratio and the propensity of the coiled-coil structure in HEWL, in the HEWL-CBB complex, and complex in the presence of an incremental concentration of ammonium sulfate, sodium chloride, ethanol, and 2-propanol (PDF)

AUTHOR INFORMATION

Corresponding Author

Ajamaluddin Malik − *Department of Biochemistry, College of Science, King Saud University, Riyadh 11451, Saudi Arabia;* orcid.org/0000-0002-5578-0652; Email: amalik@ksu.edu.sa

Authors

Javed Masood Khan − *Department of Food Science and Nutrition, College of Food and Agricultural Sciences, King Saud University, Riyadh 11451, Saudi Arabia*

Priyankar Sen − *Centre for Bioseparation Technology, VIT University, Vellore 632014, India*

Abdulaziz Alamri − *Department of Biochemistry, College of Science, King Saud University, Riyadh 11451, Saudi Arabia*

Rohit Karan − *Bioinformatics Programming Lab, Department of Biotechnology, School of Bio Sciences and Technology, VIT, Vellore 632014, India*

Arnold Emerson I − *Bioinformatics Programming Lab, Department of Biotechnology, School of Bio Sciences and Technology, VIT, Vellore 632014, India*

Complete contact information is available at: https://pubs.acs.org/10.1021/acsomega.4c10216

Author Contributions

⊥A.M., and J.M.K. contributed equally to this work. A.M., and J.M.K.: Conceptualization, data curation, formal analysis, and funding acquisition; J.M.K., A.M., A.A., P.S., R.K., and A.E.I.: investigation and methodology; J.M.K.: project administration; A.M., J.M.K., A.A., P.S., R.K., and A.E.I.: resources and software; A.M. and J.M.K.: supervision; J.M.K., A.M., A.A., and P.S.: validation; J.M.K., A.M., P.S., and A.E.I.: roles/writing—original draft; A.M., J.M.K., A.A., P.S., and A.E.I.: writing—review and editing.

Notes

The authors declare no competing financial interest.

ACKNOWLEDGMENTS

The authors are grateful to the Researchers Supporting Project number (RSPD2024R727), King Saud University, Riyadh, Saudi Arabia.

ABBREVIATIONS

CBB- Coomassie brilliant blue; HEWL- hen egg white lysozyme; MeOH- methanol; EtOH- ethanol; 2-propanol-isopropanol; FESEM- field-emission scanning electron microscope

REFERENCES

(1) Ajmal, M. R. Protein Misfolding and Aggregation in Proteinopathies: Causes, Mechanism and Cellular Response. *Diseases* **2023**, *11* (1), No. 30, DOI: 10.3390/diseases11010030.

(2) Uversky, V. N.; Fink, A. L. Conformational constraints for amyloid fibrillation: the importance of being unfolded. *Biochim. Biophys. Acta, Proteins Proteomics* **2004**, *1698* (2), 131−153.

(3) Chaudhary, A. P.; Vispute, N. H.; Shukla, V. K.; Ahmad, B. A comparative study of fibrillation kinetics of two homologous proteins under identical solution condition. *Biochimie* **2017**, *132*, 75−84.

(4) Roberts, C. J. Protein aggregation and its impact on product quality. *Curr. Opin. Biotechnol.* **2014**, *30*, 211−217.

(5) Bromley, E. H.; Krebs, M. R.; Donald, A. M. Mechanisms of structure formation in particulate gels of beta-lactoglobulin formed near the isoelectric point. *Eur. Phys. J. E* **2006**, *21* (2), 145−152.

(6) Rambaran, R. N.; Serpell, L. C. Amyloid fibrils: abnormal protein assembly. *Prion* **2008**, *2* (3), 112−117.
(7) Kastelic, M.; Kalyuzhnyi, Y. V.; Hribar-Lee, B.; Dill, K. A.; Vlachy, V. Protein aggregation in salt solutions. *Proc. Natl. Acad. Sci. U.S.A.* **2015**, *112* (21), 6766−6770.
(8) Lee, S.; Choi, M. C.; Al Adem, K.; Lukman, S.; Kim, T. Y. Aggregation and Cellular Toxicity of Pathogenic or Non-pathogenic Proteins. *Sci. Rep.* **2020**, *10* (1), No. 5120.
(9) Islam, M.; Argueta, E.; Wojcikiewicz, E. P.; Du, D. Effects of Charged Polyelectrolytes on Amyloid Fibril Formation of a Tau Fragment. *ACS Chem. Neurosci.* **2022**, *13* (21), 3034−3043.
(10) Al-Shabib, N. A.; Khan, J. M.; Malik, A.; Rehman, M. T.; Husain, F. M.; AlAjmi, M. F.; Hamdan Ali Alghamdi, O.; Khan, A. Quinoline yellow dye stimulates whey protein fibrillation via electrostatic and hydrophobic interaction: A biophysical study. *J. Dairy Sci.* **2021**, *104* (5), 5141−5151.
(11) Hakeem, M. J.; Khan, J. M.; Malik, A.; Husain, F. M.; Ambastha, V. Role of salts and solvents on the defibrillation of food dye ″sunset yellow″ induced hen egg white lysozyme amyloid fibrils. *Int. J. Biol. Macromol.* **2022**, *219*, 1351−1359.
(12) Pariary, R.; Dolui, S.; Shome, G.; Mohid, S. A.; Saha, A.; Ratha, B. N.; Harikishore, A.; Jana, K.; Mandal, A. K.; Bhunia, A.; Maiti, N. C. Coomassie brilliant blue G-250 acts as a potential chemical chaperone to stabilize therapeutic insulin. *Chem. Commun.* **2023**, *59* (52), 8095−8098.
(13) Lee, D.; Lee, E. K.; Lee, J. H.; Chang, C. S.; Paik, S. R. Self-oligomerization and protein aggregation of alpha-synuclein in the presence of Coomassie Brilliant Blue. *Eur. J. Biochem.* **2001**, *268* (2), 295−301.
(14) How, S. C.; Hsin, A.; Chen, G. Y.; Hsu, W. T.; Yang, S. M.; Chou, W. L.; Chou, S. H.; Wang, S. S. Exploring the influence of brilliant blue G on amyloid fibril formation of lysozyme. *Int. J. Biol. Macromol.* **2019**, *138*, 37−48.
(15) Carlsson, N.; Kitts, C. C.; Akerman, B. Spectroscopic characterization of Coomassie blue and its binding to amyloid fibrils. *Anal. Biochem.* **2012**, *420* (1), 33−40.
(16) Khan, J. M.; Alsenaidy, M. A.; Khan, M. S.; Sen, P.; Khan, R. H.; Fatima, S. pH induced single step shift of hydrophobic patches followed by formation of an MG state and an amyloidogenic intermediate in Lima Bean Trypsin Inhibitor (LBTI). *Int. J. Biol. Macromol.* **2017**, *103*, 111−119.
(17) Sen, P.; Fatima, S.; Ahmad, B.; Khan, R. H. Interactions of thioflavin T with serum albumins: spectroscopic analyses. *Spectrochim. Acta, Part A* **2009**, *74* (1), 94−99.
(18) Al-Shabib, N. A.; Khan, J. M.; Malik, A.; Tabish Rehman, M.; AlAjmi, M. F.; Husain, F. M.; Ahmad, A.; Sen, P. Investigating the effect of food additive dye 'tartrazine" on BLG fibrillation under in-vitro condition. A biophysical and molecular docking study. *J. King Saud Univ., Sci.* **2020**, *32*, 2034−2040.
(19) Fatima, S.; Anwar, T.; Ahmad, N.; Islam, A.; Sen, P. Non-enzymatic glycation enhances human serum albumin binding capacity to sodium fluorescein at room temperature: A spectroscopic analysis. *Clin. Chim. Acta* **2017**, *469*, 180−186.
(20) el Harith, A.; Laarman, J. J.; Minter-Goedbloed, E.; Kager, P. A.; Kolk, A. H. Trypsin-treated and coomassie blue-stained epimastigote antigen in a microagglutination test for Chagas' disease. *Am. J. Trop. Med. Hyg.* **1987**, *37* (1), 66−71.
(21) Wainwright, M.; Crossley, K. B. Methylene Blue–a therapeutic dye for all seasons? *J. Chemother.* **2002**, *14* (5), 431−443.
(22) Sharma, S.; Rathi, V. M.; Murthy, S. I.; Garg, P.; Sharma, S. Application of Trypan Blue Stain in the Microbiological Diagnosis of Infectious Keratitis-A Case Series. *Cornea* **2021**, *40* (12), 1624−1628.
(23) Chen, Y. H.; Tseng, C. P.; How, S. C.; Lo, C. H.; Chou, W. L.; Wang, S. S. Amyloid fibrillogenesis of lysozyme is suppressed by a food additive brilliant blue FCF. *Colloids Surf., B* **2016**, *142*, 351−359.
(24) Tal, M.; Silberstein, A.; Nusser, E. Why does Coomassie Brilliant Blue R interact differently with different proteins? A partial answer. *J. Biol. Chem.* **1985**, *260* (18), 9976−9980.
(25) Chial, H. J.; Thompson, H. B.; Splittgerber, A. G. A spectral study of the charge forms of Coomassie blue G. *Anal. Biochem.* **1993**, *209* (2), 258−266.
(26) Pepys, M. B.; Hawkins, P. N.; Booth, D. R.; Vigushin, D. M.; Tennent, G. A.; Soutar, A. K.; Totty, N.; Nguyen, O.; Blake, C. C.; Terry, C. J.; et al. Human lysozyme gene mutations cause hereditary systemic amyloidosis. *Nature* **1993**, *362* (6420), 553−557.
(27) Proctor, V. A.; Cunningham, F. E.; Fung, D. Y. C. The chemistry of lysozyme and its use as a food preservative and a pharmaceutical. *Crit. Rev. Food Sci. Nutr.* **1988**, *26* (4), 359−395.
(28) Krebs, M. R.; Wilkins, D. K.; Chung, E. W.; Pitkeathly, M. C.; Chamberlain, A. K.; Zurdo, J.; Robinson, C. V.; Dobson, C. M. Formation and seeding of amyloid fibrils from wild-type hen lysozyme and a peptide fragment from the beta-domain. *J. Mol. Biol.* **2000**, *300* (3), 541−549.
(29) Khan, J. M.; Chaturvedi, S. K.; Rahman, S. K.; Ishtikhar, M.; Qadeer, A.; Ahmad, E.; Khan, R. H. Protonation favors aggregation of lysozyme with SDS. *Soft Matter* **2014**, *10* (15), 2591−2599.
(30) Arnaudov, L. N.; de Vries, R. Thermally induced fibrillar aggregation of hen egg white lysozyme. *Biophys. J.* **2005**, *88* (1), 515−526.
(31) Szymańska, A.; Hornowski, T.; Slosarek, G. Denaturation and aggregation of lysozyme in water-ethanol solution. *Acta Biochim. Pol.* **2012**, *59* (2), 317−321.
(32) Sarimov, R. M.; Binhi, V. N.; Matveeva, T. A.; Penkov, N. V.; Gudkov, S. V. Unfolding and Aggregation of Lysozyme under the Combined Action of Dithiothreitol and Guanidine Hydrochloride: Optical Studies. *Int. J. Mol. Sci.* **2021**, *22* (5), No. 2710, DOI: 10.3390/ijms22052710.
(33) Malik, A.; Khan, J. M.; Alhomida, A. S.; Ola, M. S.; Alokail, M. S.; Khan, M. S.; Alenad, A. M.; Altwaijry, N.; Alafaleq, N. O.; Odeibat, H. Agitation does not induce fibrillation in reduced hen egg-white lysozyme at physiological temperature and pH. *J. Mol. Recognit.* **2023**, *36*, No. e3009.
(34) Sancataldo, G.; Vetri, V.; Fodera, V.; Di Cara, G.; Militello, V.; Leone, M. Oxidation enhances human serum albumin thermal stability and changes the routes of amyloid fibril formation. *PLoS One* **2014**, *9* (1), No. e84552.
(35) Greenfield, N. J. Using circular dichroism spectra to estimate protein secondary structure. *Nat. Protoc.* **2006**, *1* (6), 2876−2890.
(36) Rananaware, P.; Pandit, P.; Naik, S.; Mishra, M.; Keri, R. S.; Brahmkhatri, V. P. Anti-amyloidogenic property of gold nanoparticle decorated quercetin polymer nanorods in pH and temperature induced aggregation of lysozyme. *RSC Adv.* **2022**, *12* (36), 23661−23674.
(37) Konar, M.; Mathew, A.; Dasgupta, S. Effect of Silica Nanoparticles on the Amyloid Fibrillation of Lysozyme. *ACS Omega* **2019**, *4* (1), 1015−1026.
(38) Ghosh, S.; Pandey, N. K.; Singha Roy, A.; Tripathy, D. R.; Dinda, A. K.; Dasgupta, S. Prolonged glycation of hen egg white lysozyme generates non amyloidal structures. *PLoS One* **2013**, *8* (9), No. e74336.
(39) Faramarzian, M.; Bahramikia, S.; Dehghan Shasaltaneh, M. In vitro investigation of the effect of mesalazine on amyloid fibril formation of hen egg-white lysozyme and defibrillation lysozyme fibrils. *Eur. J. Pharmacol.* **2020**, *874*, No. 173011.
(40) Nemzer, L. R.; Flanders, B. N.; Schmit, J. D.; Chakrabarti, A.; Sorensen, C. M. Ethanol shock and lysozyme aggregation. *Soft Matter* **2013**, *9* (7), 2187−2196.
(41) Menard, L. M.; Wood, N. B.; Vigoreaux, J. O. Secondary Structure of the Novel Myosin Binding Domain WYR and Implications within Myosin Structure. *Biology* **2021**, *10* (7), No. 603, DOI: 10.3390/biology10070603.
(42) Lau, S. Y.; Taneja, A. K.; Hodges, R. S. Synthesis of a model protein of defined secondary and quaternary structure. Effect of chain length on the stabilization and formation of two-stranded alpha-helical coiled-coils. *J. Biol. Chem.* **1984**, *259* (21), 13253−13261.
(43) Zhou, N. E.; Kay, C. M.; Hodges, R. S. Synthetic model proteins. Positional effects of interchain hydrophobic interactions on

stability of two-stranded alpha-helical coiled-coils. *J. Biol. Chem.* **1992**, *267* (4), 2664−2670.
(44) López-García, P.; Goktas, M.; Bergues-Pupo, A. E.; Koksch, B.; Varon Silva, D.; Blank, K. G. Structural determinants of coiled coil mechanics. *Phys. Chem. Chem. Phys.* **2019**, *21* (18), 9145−9149.
(45) Fiumara, F.; Fioriti, L.; Kandel, E. R.; Hendrickson, W. A. Essential role of coiled coils for aggregation and activity of Q/N-rich prions and PolyQ proteins. *Cell* **2010**, *143* (7), 1121−1135.
(46) Lupas, A.; Van Dyke, M.; Stock, J. Predicting coiled coils from protein sequences. *Science* **1991**, *252* (5009), 1162−1164.
(47) Hicks, M. R.; Holberton, D. V.; Kowalczyk, C.; Woolfson, D. N. Coiled-coil assembly by peptides with non-heptad sequence motifs. *Folding Des.* **1997**, *2* (3), 149−158.
(48) Reichardt, C.; Welton, T. *Solvents and Solvent Effects in Organic Chemistry*; Wiley-VCH Verlag GmbH & Co. KGaA, 2010 DOI: 10.1002/9783527632220.
(49) Parry, D. A.; Fraser, R. D.; Squire, J. M. Fifty years of coiled-coils and alpha-helical bundles: a close relationship between sequence and structure. *J. Struct Biol.* **2008**, *163* (3), 258−269.
(50) Orr, H. T.; Zoghbi, H. Y. Trinucleotide repeat disorders. *Annu. Rev. Neurosci.* **2007**, *30*, 575−621.
(51) Crooks, R. O.; Rao, T.; Mason, J. M. Truncation, randomization, and selection: generation of a reduced length c-Jun antagonist that retains high interaction stability. *J. Biol. Chem.* **2011**, *286* (34), 29470−29479.
(52) Sen, P.; Ahmad, B.; Rabbani, G.; Khan, R. H. 2,2,2-Trifluroethanol induces simultaneous increase in alpha-helicity and aggregation in alkaline unfolded state of bovine serum albumin. *Int. J. Biol. Macromol.* **2010**, *46* (2), 250−254.
(53) Malik, A.; Khan, J. M.; Al-Amri, A. M.; Altwaijry, N.; Sharma, P.; Alhomida, A.; Sen, P. Hexametaphosphate, a Common Food Additive, Aggregated the Hen Egg White Lysozyme. *ACS Omega* **2023**, *8* (46), 44086−44092.

https://doi.org/10.1021/acsomega.4c10216
ACS Omega 2025, 10, 1829−1838